Am J Cancer Res 2015;5(6):2098-2112
www.ajcr.us /ISSN:2156-6976/ajcr0008133

Original Article

Endogenous Nodal promotes melanoma undergoing epithelial-mesenchymal transition via Snail and Slug *in vitro* and *in vivo*

Qiang Guo[1*], Fen Ning[1*], Rui Fang[2], Hong-Sheng Wang[1], Ge Zhang[1], Mei-Yu Quan[1], Shao-Hui Cai[3], Jun Du[1]

[1]Department of Microbial and Biochemical Pharmacy, School of Pharmaceutical Sciences, Sun Yat-Sen University, Guangzhou 510006, Guangdong, China; [2]Department of Pharmacy, Guangdong Women and Children Hospital, Guangzhou 511400, Guangdong, China; [3]Department of Pharmacology, College of Pharmacy, Jinan University, Guangzhou 510632, Guangdong, China. [*]Equal contributors and co-first authors.

Received March 17, 2015; Accepted May 10, 2015; Epub May 15, 2015; Published June 1, 2015

Abstract: Nodal, an important embryonic morphogen, has been reported to modulate tumorigenesis. Epithelial-mesenchymal transition (EMT) plays an important role in cancer metastasis. We have previously reported that recombinant Nodal treatment can promote melanoma undergoing EMT, but the effects of endogenous Nodal on EMT are still unknown. Here we generated both Nodal-overexpression and -knockdown stable cell lines to investigate the in vitro and in vivo characteristics of Nodal-induced EMT in murine melanoma cells. Nodal-overexpression cells displayed increased migration ability, accompanied by typical phenotype changes of EMT. In contrast, Nodal-knockdown stable cells repressed the EMT phenotype as well as reduced cell motility. Results of animal experiments confirmed that overexpression of Nodal can promote the metastasis of melanoma tumor in vivo. Mechanistically, we found that Nodal-induced expression of Snail and Slug involves its activation of ALK/Smads and PI3k/AKT pathways, which is an important process in the Nodal-induced EMT. However, we also found that the EMT phenotype was not completely inhibited by blocking the paracrine activity of Nodal in Nodal overexpression cell line suggesting the presence of additional mechanism(s) in the Nodal-induced EMT. This study provides a better understanding of Nodal function in melanoma, and suggests targeting Nodal as a potential strategy for melanoma therapey.

Keywords: Nodal, EMT, snail, slug, melanoma

Introduction

Nodal is an embryonic morphogen, which belongs to the transforming growth factor (TGF)-superfamily. It is an evolutionarily conserved cytokine, and plays an important role during the embryogenesis of vertebrates [1, 2]. Nodal presents high expression in the early development of vertebrate embryos, and then is gradually reduced. Its expression is barely detectable in most adult tissues, except in adult tissue stem cells and endometrium. Because embryonic development and tumorigenesis have some similar characteristics [3], Nodal may have a close relationship with the occurrence and development of tumor. Recently, it has been demonstrated that Nodal is aberrantly expressed in many aggressive tumors [4-7], but the role of Nodal in the process of tumorigenesis appears complex. Some researches suggested that Nodal induces apoptosis and inhibits proliferation of tumor cells [8, 9], while others revealed that Nodal promotes tumorigenesis [10-12]. In our early research, we found that Nodal can induce melanoma cell undergoing epithelial-to-mesenchymal transition (EMT) and then trigger the migration and invasion of cancer cells [13].

Melanoma originates in the pigment-producing melanocytes and is the most lethal skin cancers with poor prognosis [14]. It is the one of the tumors that most frequently metastasizes to distant site. The poor clinical outcome and high degree of malignancy make the melanoma a serious public health threat. Nodal is one of the factors involved in the etiology of aggressive melanomas, as its inhibition blocks the

plasticity and tumorigenic capacity of aggressive human melanoma cells [7, 15]. The molecular mechanism underlying Nodal regulation of melanomas carcinogenesis and metastasis is still unclear.

EMT is a process during which the cells lose their epithelial traits but acquire mesenchymal characteristics [16]. EMT phenotype is usually associated with down-regulation of E-cadherin, up-regulation of vimentin and fibronectin, resulting in weakened adhesion ability and enhanced motility [17]. EMT was first recognized as a feature of embryogenesis, which is vital for morphogenesis during embryonic development. In recent years, the link between EMT and tumor metastasis has been well established [18]. We have recently reported that Nodal treatment can induce melanoma cells to undergo EMT [13]. However, whether endogenous Nodal contributes to regulate EMT and the in vivo effects of Nodal on cancer metastasis are still not illustrated.

Snail, which belongs to the zinc finger transcription repressor superfamily, was first described in Drosophila melanogaster [19], where it was shown to be essential for the formation of the mesoderm [20]. In the 20 or so years since its isolation, more than 50 family members have been described in metazoans [21]. Snail and Slug (also known as Snail 2) recognize E2 box type elements (CACCTG/CAGCTG) [22, 23]. They are able to down-regulate E-cadherin expression by binding to E-boxes in the E-cadherin promoter, which makes them the key regulator of EMT [24]. In this study, by using Nodal-related stable cell lines combined with Snail and Slug overexpression and silencing, we demonstrated that Snail and Slug are the key factor in the Nodal-induced EMT process.

Materials and methods

Chemicals and reagents

Small molecule inhibiting agents SB431542, LY294002, and primary antibodies against Nodal and vimentin were obtained from Santa Cruz Biotechnology Inc. (Santa Cruz, CA, USA). Primary antibodies against E-cadherin, Snail, Smad2, p-Smad2, Akt, p-Akt (Ser473), GSK-3, p-GSK-3. (Ser9) were purchased from Cell Signaling Technology (MA, USA). Rabbit poly antibodies to α-tubulin and GAPDH were obtained from Boster Biological Engineering (Wuhan, China). Horseradish peroxidase (HRP) or FITC/Rhodamine B-conjugated goat anti mouse/rabbit IgG polymer were obtained from Biosynthesis Biotechnology (Beijing, China). DAB were obtained from ZhongShan Gloden-Bridge (Beijing, China). Recombinant mouse Nodal protein was purchased from R&D Systems (Minneapolis, USA). PrimeScript® RT reagent Kit and SYBR® Premix Ex Taq™ were products of TaKaRa. E.Z.N.A® HP Total RNA Kit was bought from Omega Bio-Tek (Norcross, GA, USA). The DAPI dye, Lipofectamine 2000 and Puromycin were purchased from Invitrogen (Carlsbad, CA, USA). G418 was from Biovision (Palo Alto, CA, USA). Nodal neutralizing antibody (rabbit polyclonal antibody) was produced by our own laboratory [25].

Cell culture and gene transient transfection

B16 cell line was obtained from the The Cell Bank of Type Culture Collection of the Chinese Academy of Sciences (Shanghai, China). The cells were maintained in RPMI1640 culture medium (Gibco BRL) containing 10% fetal bovine serum, 2 mM L-glutamine and incubated under a humidified 5% CO_2 atmosphere at 37°C. Before transfection, B16 cells were seeded on a 6-well plate (1.5×10^5 cells/well), left to grow to 80~90% confluence. They were then transfected with 2 μg plasmid vector or 100 pmol small interfering RNAs (siRNAs) oligomer targeting specific genes (Invitrogen) per well mixed with lipofectamine 2000 reagent in serum reduced medium according to the manufacturer's instructions. Medium was changed to complete culture medium 6 h later, and the cells were incubated at 37°C in a CO_2 incubator for another 24 to 48 h before harvest. Transfection efficiency was normalized by transfection with pEGFP-N3 or Fluorescent Oligo (Cat. No. 2013, Invitrogen).

Generation of B16/pldNodal and B16/shNodal cells

The murine Nodal expression vector used for generation of Nodal overexpression cell line was constructed as previously described [26]. Briefly, the murine Nodal gene was cloned into a 2A peptide-linked multicistronic vector pL-tdTomato-Neo, which was kindly donated by Dr. Changmin Chen from Harvard Medical School, to generate the plasmid pL-tdTomato-mNodal,

in which the red fluorescent protein, Nodal and resistance genes were serially linked by two 2A peptide genes [27, 28]. The Nodal silencing shRNA plasmids pGFP-V-RS-Nodal was purchase from Origene (TR TG501492, OriGene Technologies). The shRNA targeted mouse Nodal gene sequences is 5'-GGTCAAGTTCCAGGTGGACTTCAACCTGA-3'

Before transfection, B16 cells were seeded onto a 6-well plate (1.5×10^5 cells/well) and allow to grow to 80~90% confluency. The plasmid pL-tdTomato-mNodal or pGFP-V-RS-Nodal was introduced into the cells via liposome-mediated transfection. Expression of the red and the green fluorescence proteins in these two vectors were used to monitor transfection efficiency. The transfected B16 cells were selected with G418 (700 μg/ml for pLd-Nodal) or puromycin (1 μg/ml for psh-Nodal) for 10~14 days. The survived cells were picked out and seeded into 96-well plate for formation of cell clones and further expansion. The expanded monoclonal cell populations were named as B16-pldNodal and B16-shNodal, respectively. The mock cells transfected with pL-tdTomato-Non or pGFP-V-RS-scrambled Non-Effective (TR30013, OriGene Technologies) were named as B16-pldMock or B16/shMock. The morphous and fluorescence intensity of the cells were observed under inverted fluorescence microscope. Cell proliferation activity was determined by MTT assay [29].

Quantitative Real-Time PCR

Total mRNA of the cells was extracted for detection of transcription levels of different genes. First strand cDNA was synthesized from 500 ng of total RNA. Quantification of target and reference (Gapdh) genes was performed in triplicate on LightCycler® 480 II (Roche, Applied Science). The primers used in each reaction were as follows: Nodal (NM_013611.4), F: 5'-TACATGTTGAGCCTCTACCGAGACC-3' and R: 5'-AAACGTGAAAGTCCAGTTCTGTCC-3'; E-cadherin (NM_011427.2), F: 5'-CGTCCTGCCAATCCTGATGA-3' and R: 5'-ACCACTGCCCTCGTAATCGAAC-3'; Vimentin (NM_009864.2), F: 5'-AAAGCGTGGCTGCCAAGAAC-3' and R: 5'-GTGACTGCACCTGTCTCCGGTA-3'; Snail (NM_011701.4), F: 5'-TCTGAAGATGCACATCCGAAGC-3' and R: 5'-TTGCAGTGGGAGCAGGAGAAT-3'; Slug (NM_011415.2), F: 5'-CTCACCTCGGGAGCATACAGC-3' and R: 5'-TGAAGTGTCAGAGGAAGGCGGG-3'; GAPDH (NM_008084.2), F: 5'-TGTGTCCGTCGTGGATCTGA-3' and R: 5'-TTGCTGTTGAAGTCGCAGGAG-3'. Following normalization to GAPDH gene, expression levels for each target gene were calculated using the comparative threshold cycle (CT) method. Data were analyzed using optical system software version 3.1 (Bio-Rad) and to generate relative expression values. The Δct values were calculated according to the formula Δct = ct (gene of interest)-ct (Gapdh) in correlation analysis, and the $2^{-\Delta\Delta ct}$ was calculated according to the formula ΔΔct = Δct (control group)-Δct (experimental group) for determination of relative. Data is presented as the mean ± standard deviation (SD) from three independent experiments.

Western blotting analysis

Western blotting assays were performed as previously described [30]. For signal pathway analysis, the cells were pre-treated with inhibitors against AKT (10 μM LY294002), ALK (10 μM SB431542), or the vehicle (DMSO) for 1h, and the whole cell protein extracts were prepared, quantified and subject to SDS-PAGE and immunoblotting.

Immunofluorescence microscopy

The B16-pldNodal, B16-shNodal and parental cells were seeded on chamber slides (10^4/ml), serum starved overnight. The cells were fixed with 4% paraformaldehyde for 20 min and blocked with 10% normal goat serum in PBS for 45 min at 37°C, then incubated with antibodies against Nodal (1:100 dilution), E-cadherin (1:100 dilution), vimentin (1:100 dilution) and Snail (1:100 dilution) at 4°C overnight. Slides were washed three times with PBS and incubated with FITC or Rhodamine B-conjugated secondary antibodies (1:1000 dilution) for 45 min at 37°C. Then, the cells were counter stained with DAPI (10 μg/ml) for 10 min and were examined with Confocal Laser Scanning Microscopy (Zeiss) for analysis of Snail nuclear translocation.

Wound healing scratch assay

The B16-pldNodal, B16-shNodal and parental cells were grown as monolayers in triplicates in 24-well plates (1×10^5/well) until confluent, and were serum starved overnight. An artificial scratch wound was created, and the cell debris

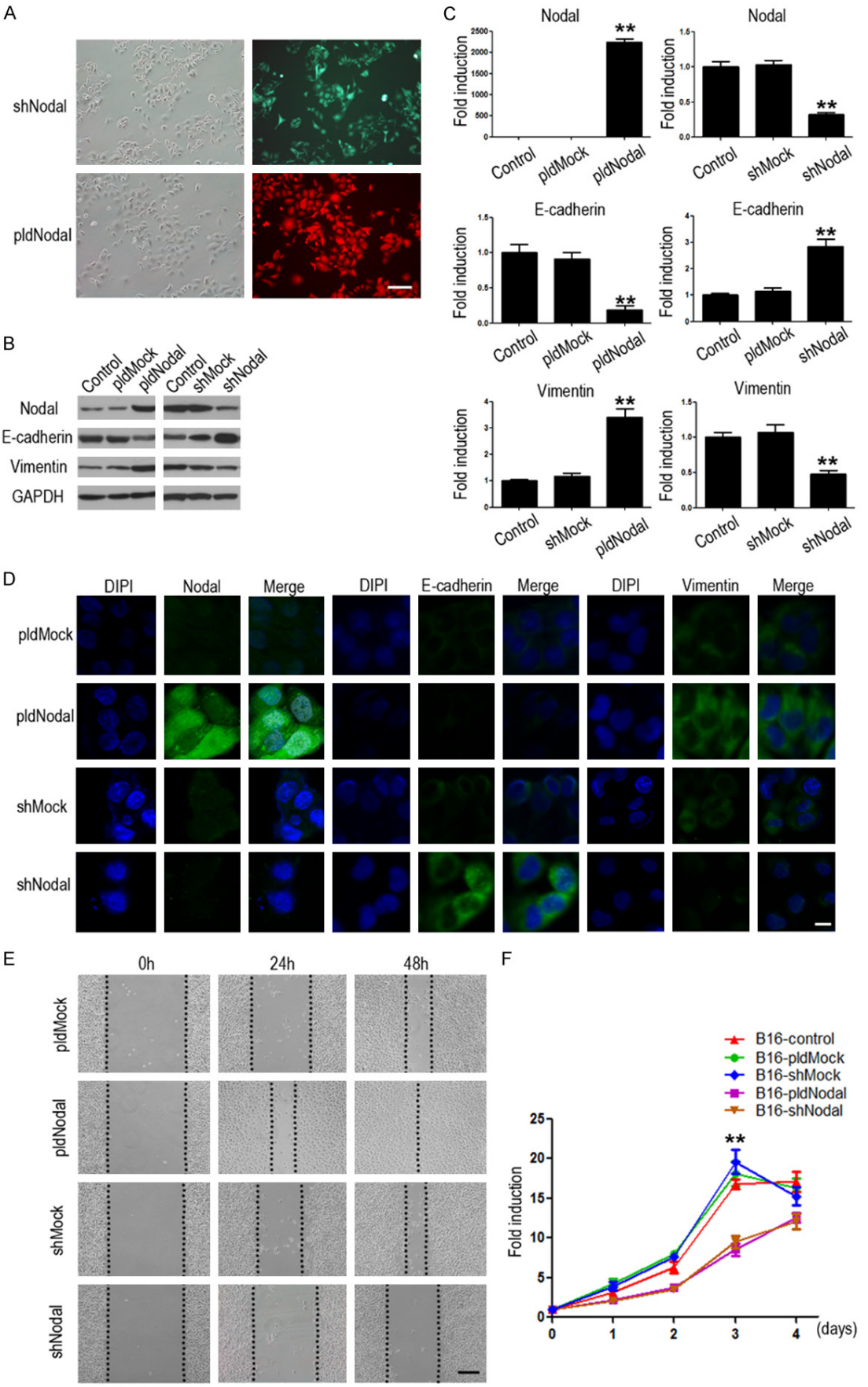
A
shNodal
pldNodal
B
Control
pldMock
pldNodal
Control
shMock
shNodal
Nodal
E-cadherin
Vimentin
GAPDH
C
Nodal
Fold induction
Control
pldMock
pldNodal
Nodal
Control
shMock
shNodal
E-cadherin
Vimentin
D
DIPI
Nodal
Merge
E-cadherin
Vimentin
pldMock
pldNodal
shMock
shNodal
E
0h
24h
48h
F
B16-control
B16-pldMock
B16-shMock
B16-pldNodal
B16-shNodal
Fold induction
(days)

Figure 1. Stable murine melanoma B16 cell lines with Nodal overexpressed and knockdown were established by transfection pL-tdTomato-mNodal and pGFP-V-RS-Nodal, named B16-pldNodal and B16-shNodal. (A) B16-pldNodal cells emit red glow while B16-shNodal cells emit green glow. Scale bar, 50 m. The protein (B) and mRNA (C) levels of Nodal, E-cadherin and vimentin were detected with Western blotting analysis and qRT-PCR in B16-pldNodal cells and B16-shNodal cells respectively, Comparing with each parent cells and Mock cells. (D) Expression and location of Nodal, E-cadherin and vimentin in each B16 stable cell lines was determined by immunofluorescence. Scale bar, 20 m. (E) Representative phase-contrast images of each B16 stable cell lines migrating into wounded area at 24 h and 48 h after scratch injury. Scale bar, 50 m. (F) The growth curve of each B16 stable cell lines was determined by MTT (*P<0.01; **P<0.001).

was removed by washing with PBS. The migration of these cells was photographed 24 to 48 h later. In cell co-culture system, the same number of B16-pldNodal and B16-shNodal cells were mixed and seeded in 24-well plates (0.5×10^5/well per cell line), then the cell migration was observed with inverted fluorescence microscope. In signal pathway blocking assay, the cells were cultured in media supplemented with LY294002 or SB431542 or a function-blocking rabbit anti-Nodal antibody (2 μg/ml), and the healing process was monitored all along. For most experiments, these antagonists were diluted in complete RPMI and added to cells daily for a period of 48-72 h. Each assay was carried out in triplicate and repeated in three independent experiments.

Mouse melanoma subcutaneous graft tumor model

C57BL/6 mice aged 6-8 weeks were purchased from the Medical Experimental Animal Center of Guangdong Province (Guangzhou, China). Eight mice from each group were inoculated subcutaneously in the right axillary spaces with cells B16/pldNodal, B16/pldMock, B16/shNodal, and B16/shMock respectively at 1×10^5/mouse. Tumor length (L) and width (W) were measured every other day and tumor volume was calculated as $(L \times W^2) \times 0.4$. At the end of the experiment, the mice were sacrificed, and the tissue samples including tumor, lung and liver were immediately washed with PBS and fixed in 10% neutral-buffered formalin solution for 2-3 days. The fixed tissue was dehydrated and embedded in paraffin. Sections (4 μm) were subjected to routine hematoxylin-eosin (H&E) staining or immunohistochemistry for histological and pathological analysis. The experiments were approved by the Sun Yat-sen University Animal Care and Use Committee and conducted in accordance with the provisions of the Declaration of Helsinki.

Immunohistochemistry

Sections from allograft tumors were subjected to deparaffinization/rehydration, and antigen retrieval with boiling in 0.01 M sodium citrate buffer (pH 6.0) for 30 min. The sections were blocked with 10% goat serum, and incubated with the primary antibodies against Nodal, E-cadherin, fibronectin, vimentin, MMP-2, and Snail at a dilution of 1:200 at 4°C overnight in a humidified chamber. After washing with PBS for three times, slides were incubated with goat anti mouse/rabbit HRP-conjugated antibody, and DAB was applied as substrate. Mayer's hematoxylin was used as a counter stain. Throughout the above analyses, controls were prepared by omitting the primary antibodies.

Statistical analysis

Results are expressed as mean ± SD of three independent experiments unless otherwise specified. Data were analyzed by two-tailed unpaired Student's t-test between any two groups. One-way ANOVA analysis of variance was used to assess the difference of means among groups. These analyses were performed using GraphPad Prism Software Version 5.0 (GraphPad Software Inc., La Jolla, CA). P<0.05 was considered statistically significant.

Results

Generation of Nodal overexpression and knockdown B16 melanoma stable cell lines

To facilitate characterization of Nodal-induced EMT process, we first set to establish Nodal overexpression (B16-pldNodal) and knockdown cell lines (B16-shNodal). B16-pldNodal can emit red glow under 650 nm excitation, while B16-shNodal can emit green glow under 540 nm excitation light (**Figure 1A**). we examined the expression of Nodal and EMT related markers in each stable cell line using Western blotting (**Figure 1B**), qRT-PCR (**Figure 1C**) and

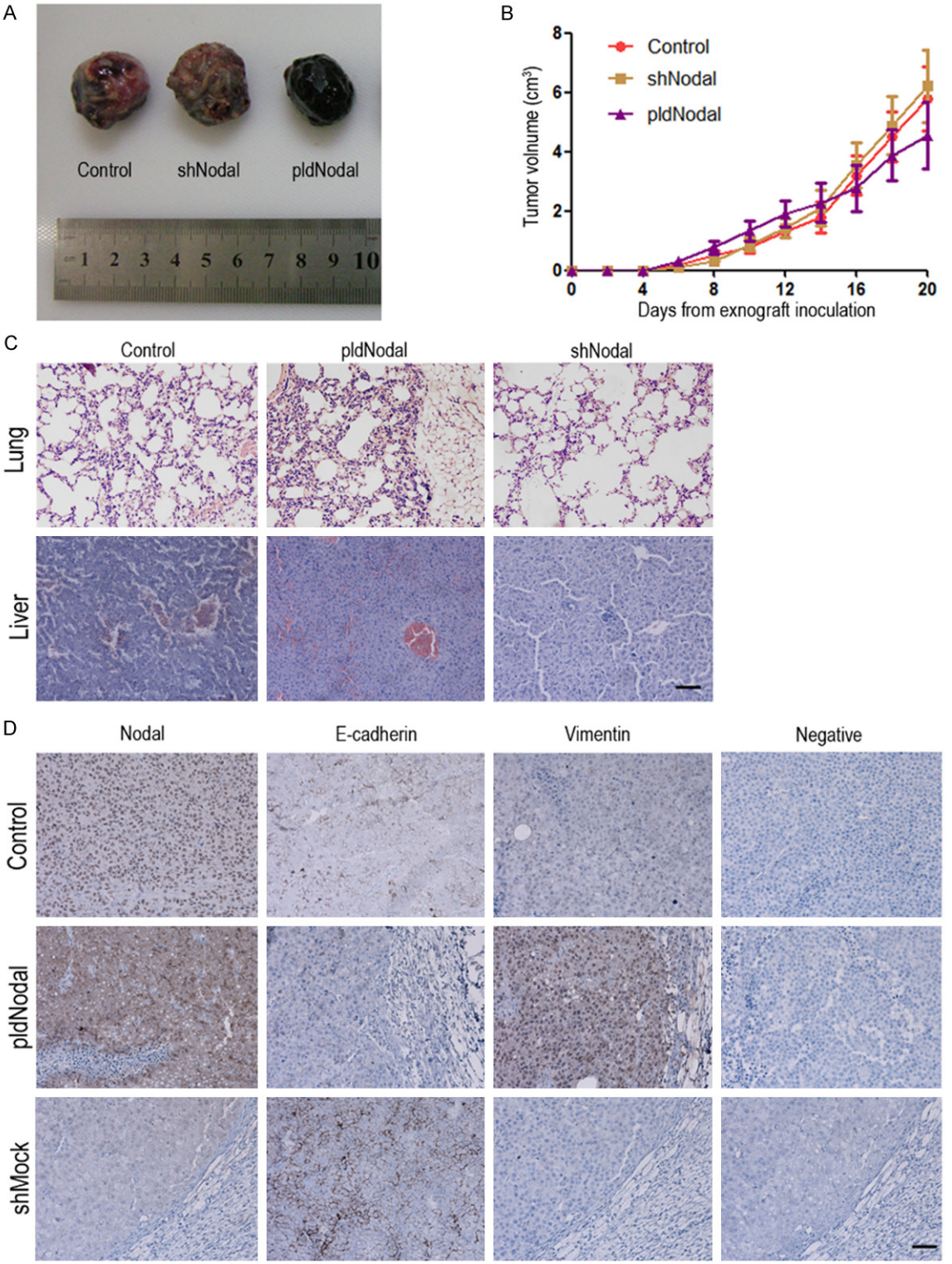

Figure 2. Overexpressed or silenced Nodal affect tumorigenic capacity and tumor metastasis in vivo. C57BL/6 mice were transplanted with 4 × 10^5 of each B16 cell lines cells respectively with i.p. injection. A. Represen tative macroscopic appearance of each B16 cell lines allograft. B. Values represent the median tumor volume. C. H&E examination of each B16 cell lines metastasis in lung and liver tissue section. Scale bar, 50 m. D. The tumor tissue sections were subjected to IHC detection of Nodal, E-cadherin and vimentin. Scale bar, 50 m.

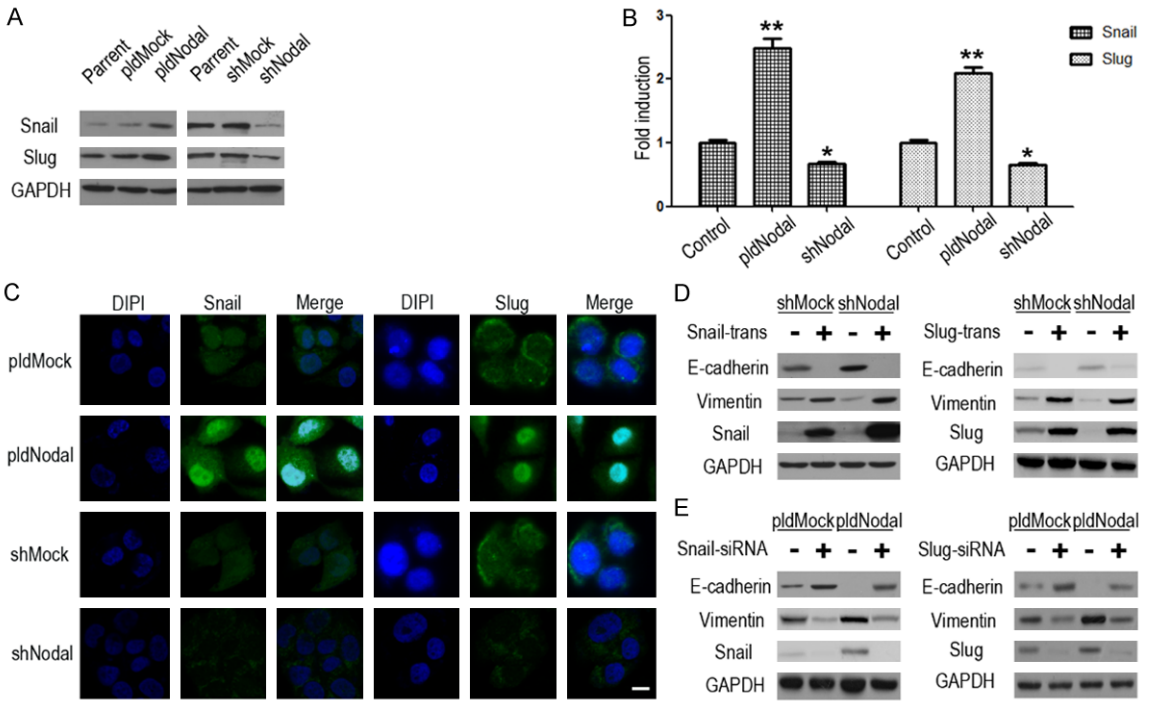

Figure 3. Snail and Slug are crucial in the EMT process of B16-pldNodal and B16-shNodal. The protein (A) and mRNA (B) levels of E-cadherin, vimentin, Snail and Slug were detected by Western blotting analysis and qRT-PCR. (C) The expression and location of Snail and Slug in B16-pldNodal, B16-shNodal and each of their Mock cell lines were determined by immunofluorescence. Scale bar, 20 m. (D) Each B16 cells lines cells were transfected with no-load pCMV plasmid or pCMV-Snail/pCMV-Slug plasmid for 24 h, and then collected the protein for Western blotting analysis. (E) Each B16 cells lines cells were transfected with non-targeting control siRNA or Snail/Slug specific siRNA for 24 h, and then collected the protein for Western blotting analysis (**P*<0.01; ***P*<0.001).

immunofluorescence assay (**Figure 1D**), Nodal and vimentin were up-regulated and E-cadherin was down-regulated in B16-pldNodal cells, while Nodal and vimentin were down-regulated and E-cadherin was up-regulated in B16-shNodal cells confirming that stable cell lines were successfully generated and the results matched the expected changes in EMT. We next analyzed the ability of migration of the stable cell lines with wound healing scratch assay. We found that B16-pldNodal cells showed an enhanced ability of migration, while B16-shNodal cells showed a weaker ability of migration (**Figure 1E**). We also analyzed the proliferation ability of each cell line. Interestingly, both B16-pldNodal cells and B16-shNodal cells showed reduced ability in proliferation (**Figure 1F**).

Effects of overexpression or silencing Nodal on tumorigenic capacity and tumor metastasis in vivo

The above results revealed that Nodal plays an important role in the invasiveness of melanoma cells *in vitro*. We next further investigated the effect of Nodal on tumorigenic capacity and tumor metastasis *in vivo*. B16 cells, B16-pldNodal cells and B16-shNodal cells were inoculated into C57BL/6 mice, followed by tumor measurements on alternate days for 3 weeks. The tumor growth was monitored and the primary tumor, lung, and liver tissue were collected after termination of the experiments for histological and pathological analysis. There we observed no significant difference in tumor growth between different cell lines (**Figure 2A** and **2B**). The histological results showed that the ability to form secondary tumors in lung, but not liver, is enhanced in B16-pldNodal cells and is weakened in B16-shNodal cells (**Figure 2C**). These results indicated that Nodal mainly affect cell invasion, but not proliferation, of B16 cells *in vivo*.

We further determined the expression of Nodal and epithelial/mesenchymal markers in tumor tissues to investigate if the EMT phenotype of B16 cells was influenced by Nodal *in vivo*. Tumors derived B16-pldNodal cells displayed higher expression of Nodal as expected, they also showed increased expression of vimentin

and decreased expression of E-cadherin. On the contrary, tumors derived from B16-shNodal cells displayed lower expression of Nodal and vimentin and but higher expression of E-cadherin (**Figure 2D**).

Snail and Slug are crucial for Nodal-induced EMT

EMT can be driven by a set of transcriptional factors including the zinc-finger proteins Snail/Slug [31, 32]. In this study, we detected fluctuation in mRNA and protein levels of those transcriptional factors in Nodal overexpression and silence cells lines. Snail and Slug were both significantly up-regulated in B16-pldNodal cells, while significantly decreased in B16-shNodal cells (**Figure 3A** and **3B**). Further, a significant increase in nuclear translocation of Snail and Slug was observed in B16-pldNodal cell, which was inhibited in B16-shNodal cells (**Figure 3C**). The above results demonstrated that Nodal can not only up-regulate Snail protein at transcriptional level, but also promote its nuclear translocation activity during EMT induction.

We performed overexpression and knockdown assays to verify whether Snail and Slug is key regulators in Nodal-induced EMT. Results showed that overexpress either Snail or Slug can up-regulate vimentin and down-regulate E-cadherin (**Figure 3D**), further, knockdown either Snail or Slug can down-regulate vimentin and up-regulate E-cadherin in each B16 cells (**Figure 3E**). Collectively, our results showed that Snail and Slug are crucial for Nodal-induced EMT.

Nodal up-regulates Snail and Slug partly via ALK/Smads and PI3k/AKT pathways

ALK4/7 is the major receptor of Nodal. Smad2 and Smad3 will be phosphorylated while ALK4/7 is activated by Nodal [33]. The phosphorylated Smads proteins form heteromeric complexes with Smad4 and translocate into the nucleus to activate the transcription function, including active *Snail/Slug* transcriptional activity [34]. In the present study, Smad2 was phosphorylated in B16-pldNodal cells and dephosphorylated in B16-shNodal cells (**Figure 4A**). Further, SB431542, a specific inhibitor of ALK4/5/7, can prevent the phosphorylation of Smad2 and down-regulated Snail and Slug via a time dependent manner, which in turn reverses the mesenchymal phenotype of B16-pldNodal (**Figure 4B**). SB431542 also obviously inhibited the migratory capability of B16 cells in wound healing scratch assay (**Figure 4D**).

PI3k/AKT pathway is activated upon TGF-β stimulation during EMT [35]. We also found that PI3k/AKT pathway played important role in recombinant-Nodal-induced EMT [13]. Therefore we examined whether PI3k/AKT pathway is involved in the endogenous-Nodal-induced EMT. AKT is highly phosphorylated in B16-pldNodal cells and dephosphorylated in B16-shNodal cells (**Figure 4A**). Blocking ALK pathway with SB431542 would also inhibit the phosphorylation of AKT, suggesting a crosstalk between ALK pathway and PI3k/AKT pathway during this process. GSK-3 is a kinase located downstream of the PI3K/AKT pathway, which maintains an active state (Dephosphorylating) in resting epithelial cells and promotes Snail nuclear export and cytoplasmic degradation [36, 37]. In this study, we found that GSK-3 was also high phosphorylated, which means inactivation, in the B16-pldNodal cells (**Figure 4C**).

To confirm the crucial role of AKT pathway in Nodal-induced EMT, a specific antagonist of PI3k/AKT pathway, LY294002 [38] was used. B16-pldNodal cells were treated with LY294002 via a time dependent manner. LY294002 significant inhibit the phosphorylated level of AKT and GSK-3. The induction of Snail/Slug and mesenchymal marker (vimentin) as well as repression of epithelial marker (E-cadherin) by Nodal was conversed by inhibiting AKT activity (**Figure 4C**). And LY294002 also obviously inhibited the migratory capability of B16 cells in wound healing scratch assay (**Figure 4D**). EGF is a strong PI3k/AKT pathway activator [39]. As the inhibition of ALK pathway result in dephosphorylated of AKT, we want to know whether the effects of ALK4/7 inhibition would be rescued via activating AKT. B16-pldNodal cells were treated with SB431542 and EGF, and then, the protein level of pSmad2, Smad2, pAKT, AKT, vimentin, E-cadherin, Snail and Slug were detected. The results showed that activating AKT would partly reverse the effects of SB431542 (**Figure 4E**).

Regulation loop between Snail and Slug during Nodal-induced EMT

The effects of SB431542 and LY294002 on mRNA levels of E-cadherin, vimentin, Snail and

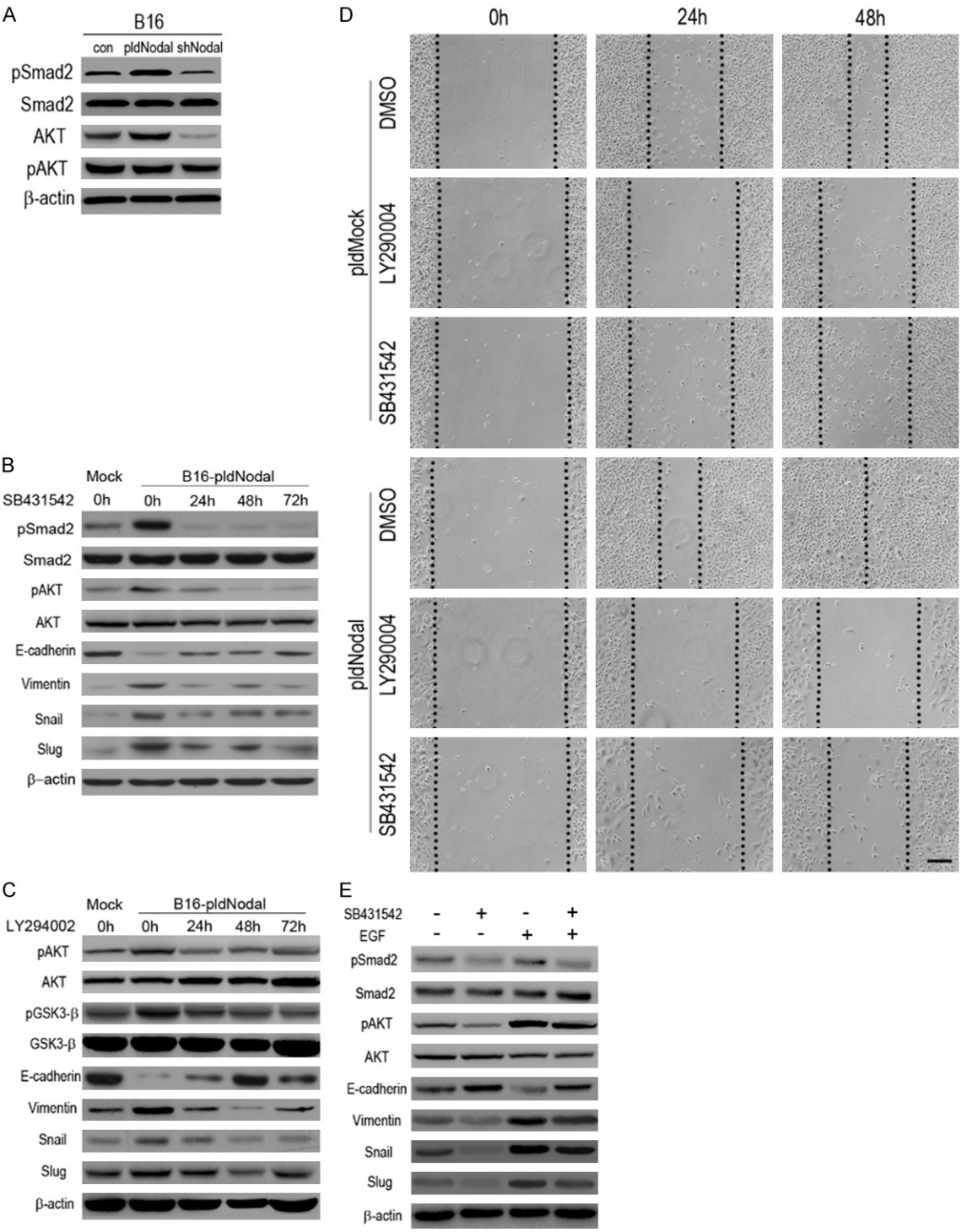

Figure 4. Nodal up-regulates Snail and Slug partly via activation of ALK/Smads pathway and PI3k/AKT pathway. A. The protein of B16 cells, B16-pldNodal cells and B16-shNodal cells were collected for Western blotting analysis to test the activity of ALK pathway and PI3k/AKT pathway. B. B16-pldMock cells and B16-pldNodal cells were treating with SB431542 (10 mM) in a time dependent manner, and then the protein was collected for Western blotting analysis. C. B16-pldMock cells and B16-pldNodal cells were treat with LY2940002 (10 mM) in a time dependent manner, and then the protein was collected for Western blotting analysis. D. B16-pldNodal cells and B16-pldMock cells were treated with SB431542 (10 mM) or LY29004 (10 mM) overnight, controlled by DMSO, and then subjected to wound healing scratch assay. Cells were accompanied by SB431542 or LY29004 treatment over the experiment. Scale bar, 50 m. E. B16-pldNodal cells were treated with SB431542 (10 mM) or EGF (100 ng/ml) for 24 h, and then the protein was collected for Western blotting analysis.

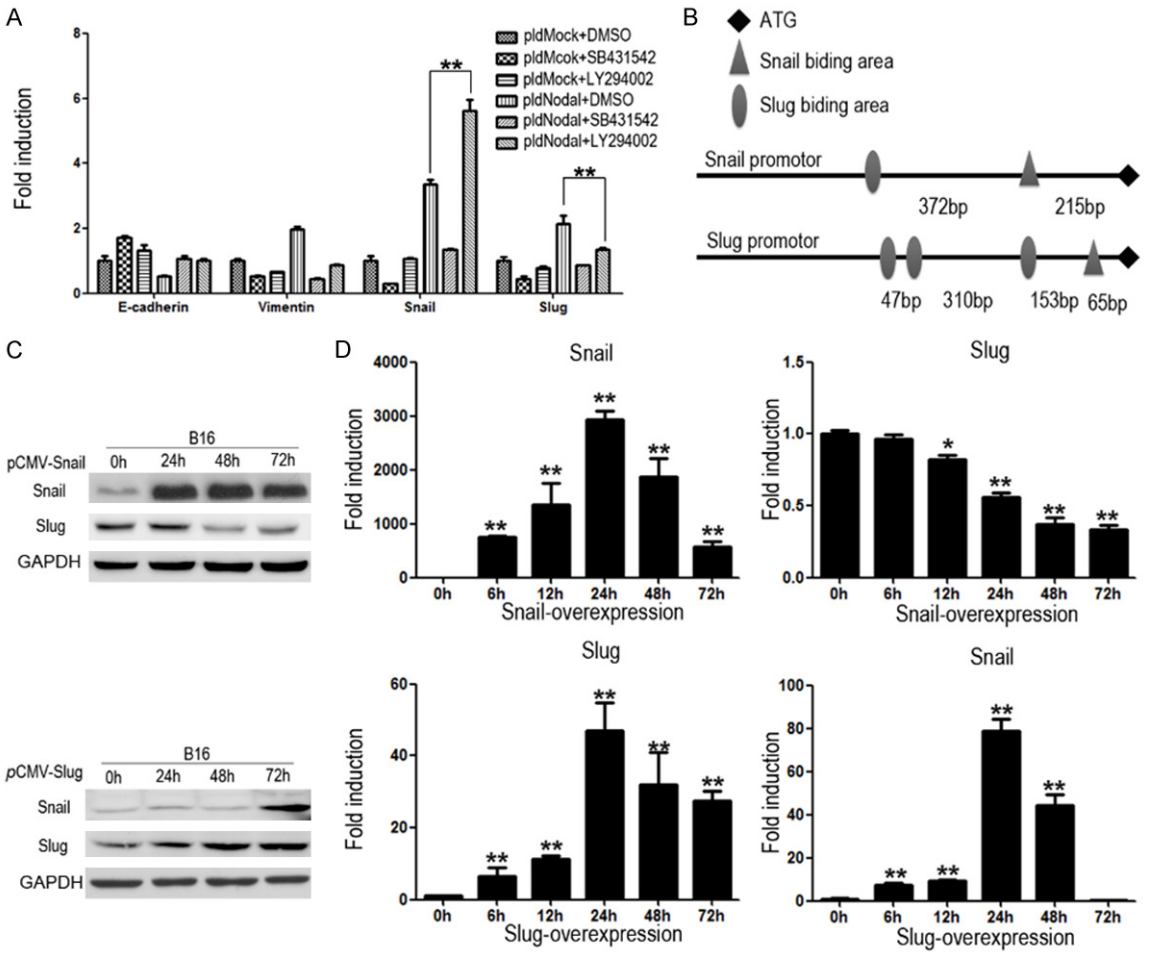

Figure 5. There is interaction mechanism between Snail and Slug during EMT process. (A) B16-pldMock cells and B16-pldNodal cells were treated with DMSO, SB431542 (10 mM) or LY29004 (10 mM) for 24 h. The mRNA was collected for qRT-PCR. (B) Promoter information of Snail and Slug from PubMed. B16 cells were transfected with pCMV-Slug or pCMV-Snail in a time dependent manner, and the protein and mRNA were collected for Western blotting analysis (C) and qRT-PCR (D) (*P<0.01; **P<0.001).

Slug were quantified by qRT-PCR. Unexpectedly, LY294002 significantly up-regulated the RNA level of Snail (**Figure 5A**), which is not fit with the protein results. Peiro et al proved that Snail can bind to its own promoter and suppress its expression [40]. Another study revealed that Slug can induce its own expression [41]. So, we assumed that there has the same mechanism in B16 cells. We searched the promoter information of *Snail* and *Slug* on the PubMed, and found that there are one Slug binding E-box sequence (CAGCTG) and one Snail binding E-box sequence (CACCTG) on the promoter of *Snail*, and three Slug binding E-box sequences and one Snail binding E-box sequences on the promoter of Slug (**Figure 5B**). We overexpressed Snail and Slug in B16 cells respectively, and found that Snail can down-regulate Slug and Slug can up-regulate Snail in both protein (**Figure 5C**) and RNA levels (**Figure 5D**). Above all, the results proved that there is a regulation loop between Snail and Slug, which suggests a complex regulation network during the Nodal-induced EMT.

EMT is not completely inhibited by blocking the paracrine of Nodal

As Nodal is a secreted cytokine, we use Nodal anti-body (abNodal) to neutralize the Nodal in the medium. Unexpected, abNodal can inhibit the migration capacity of all of the cell lines, but B16-pldNodal cells still exerted a higher migration capacity (**Figure 6A**). To confirm this

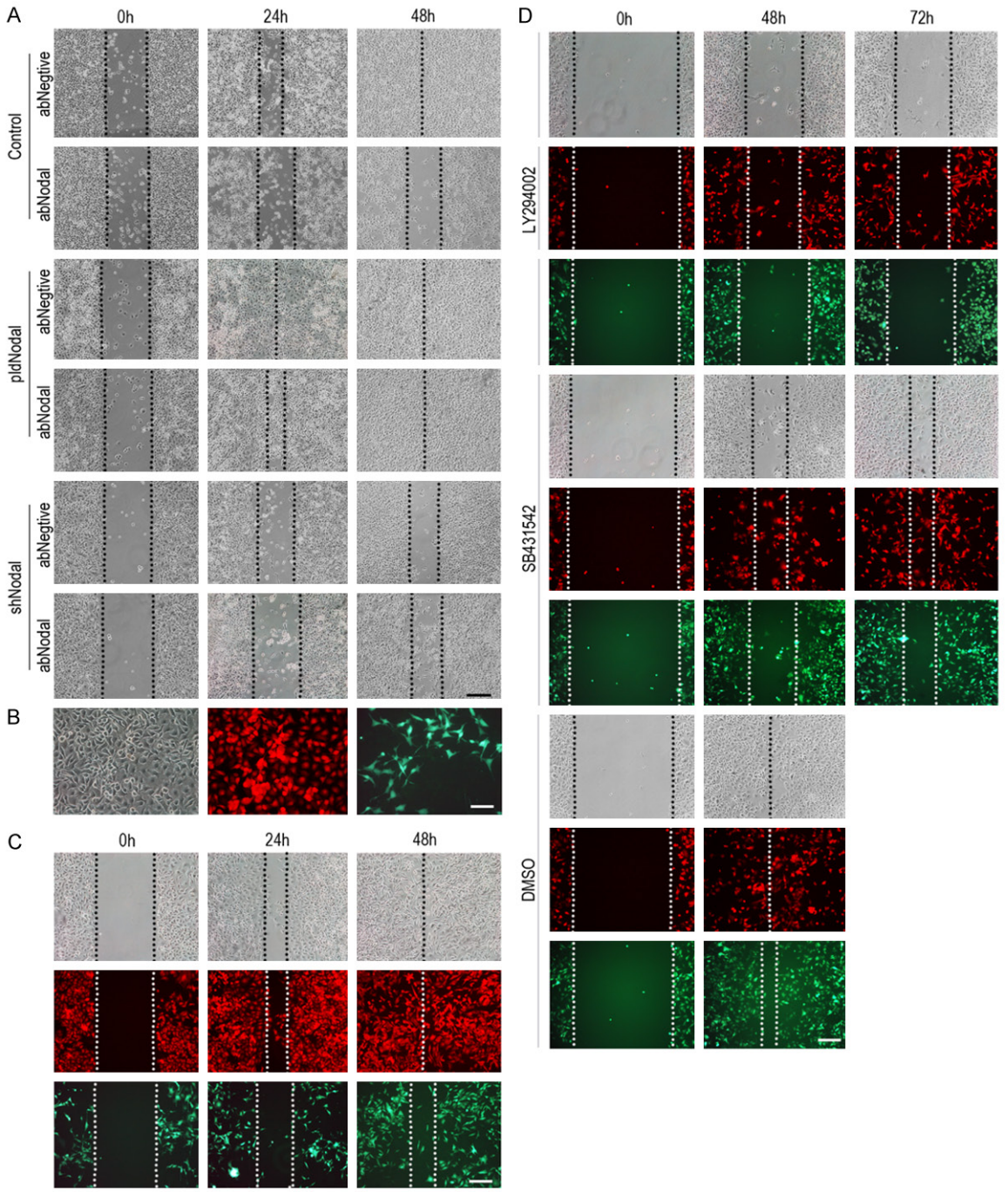

Figure 6. EMT is not completely inhibited by blocking the paracrine of Nodal. A. B16, B16-pldNodal cells and B16-pldMock cells were treated with Nodal neutralizing antibody (rabbit polyclonal antibody) overnight, controlled by rabbit serum, and then subjected to wound healing scratch assay. Cells were accompanied by Nodal neutralizing antibody over the experiment. B. B16-pldNodal cells and B16-shNodal cells were 1:1 mixed, and co-cultured for 28 days and then mixed cells were observed by fluorescence microscope. B16-pldNodal emit red light and B16-shNodal emit green light. C. The mixed cells were subjected for wound healing scratch assay. D. The mixed cells were treated with SB431542 (10 mM) or LY29004 (10 mM) overnight, controlled by DMSO, and then subjected to wound healing scratch assay. Cells were accompanied by SB431542 or LY29004 treatment over the experiment. Scale bar: 50 m in A-D.

result, we co-cultured B16-pldNodal and B16-shNodal cells for 28 days. After 28 days co-culture, there are still differences in morphology between B16-pldNodal cells (red) and

B16-shNodal cells (green) (**Figure 6B**). And then, the mixed cells were subjected to wound healing scratch assay. The B16-pldNodal cells (red) migrated further than it cultured alone (compare **Figures 1E** and **6C**), but the B16-pldNodal cells (red) migrated further than the B16-shNodal cells (green) (**Figure 6C**). SB431542 and LY294002 were added respectively to analyze whether ALK/Smads or the PI3k/AKT pathway was involved in this process. Compared with DMSO, both SB431542 and LY294002 significantly inhibited the migration capacity of the mix cells, but the B16-pldNodal cells (red cells) still migrated further than the B16-shNodal cells (green cells) (**Figure 6D**). These results overturn our perception of secreted cytokine, and the mechanism needs further research.

Discussion

EMT is an important process during early embryogenic morphogenesis. And Nodal is also an embryonic morphogen which is barely detectable in most adult tissues and re-express in many aggressive tumor. This suggested that there may be close relationship between the Nodal and EMT. In this study, we built Nodal overexpression cell line B16-pldNodal and Nodal knockdown cell line B16-shNodal to research the relationship of Nodal and EMT. The *in vitro* experiments proved that B16-pldNodal cells show more mesenchymal phenotype and stronger migration capability than B16-shNodal cells and mock cells. And we found a very interesting phenomenon that either B16-pldNodal cells or B16-shNodal cells show a restrained ability in proliferation compared with each of their mock cells and parent cells. Up to now, there is still a dispute in the influence of Nodal to cell proliferation. Some results supported that Nodal promotes cell proliferation [42-44], while other results suggested that Nodal inhibits cell proliferation [8, 45, 46]. On the basis of our results, maybe the concentration of Nodal is the key to Nodal-related proliferation. But in the animal experiments, tumors derived from B16-shNodal and control cells display no significant difference in volume. A possible reason is that B16-shNodal cells lack the ability of migration, and tends to stay at primary lesion.

We further used an allograft mouse model to further investigate the relationship between Nodal expression and the epithelial/mesenchymal phenotype in promoting the invasive and metastatic potential of melanoma cells. The results showed that B16-pldNodal cells show a very strong capability of pulmonary metastasis, while B16-shNodal cells are very few to the lung. This was supported by results of immunohistochemistry. The sections of B16-pldNodal tumor tissue was detected high vimentin expression and low E-cadherin expression, while the sections of B16-shNodal showed an opposite results. Hence, the present study showed for the first time that Nodal can promote tumorigenesis by inducing EMT, but not promote proliferation, in B16 murine melanoma cells and thereby favoring invasion and metastatic potential of the tumor *in vivo*. These observations supported the notion that Nodal expression is associated with the acquisition of aggressive phenotype in B16 melanoma, and that inhibiting Nodal signaling may be a novel therapeutic strategy for melanomas.

In present study, we demonstrated that Snail and slug is the key regulator to the Nodal-induced EMT. Knockdown of either Snail or Slug abolished Nodal-induced EMT marker changes in B16 cells. ALK/Smads pathway and PI3k/AKT pathway which are both active in B16-pldNodal cells and inactive in B16-shNodal cells is the two key signaling pathways to regulate Snail and Slug. Either inhibited ALK/Smads pathway or inhibited PI3k/AKT pathway reduced the expression of vimentin, Snail and Slug, and promoted the expression of E-cadherin in B16 cells, which weaken the migration capability of B16 cells. But, the mechanism that induce Snail and Slug of those two pathways is different. The complexes of Smads can translocate into the nucleus to activate the transcription of *Snail* and *Slug* [34], While activated pAKT can stable the protein level of Snail and Slug through inactivate GSK-3 [37]. So, inhibiting ALK/Smads pathway can suppress the mRNA level of Snail and Slug, but inhibiting PI3k/AKT cannot get the same result. In fact, inhibits PI3k/AKT pathway will lead up-regulated the mRNA level of Snail, especially in B16-pldNodal cells. This may be caused by negative feedback mechanism of Snail, as Snail can bind to its own promoter and suppress its expression (Figure S1) [40]. When PI3k/AKT pathway is inhibited, the Snail protein will be very unstable and degraded rapidly, so the suppression

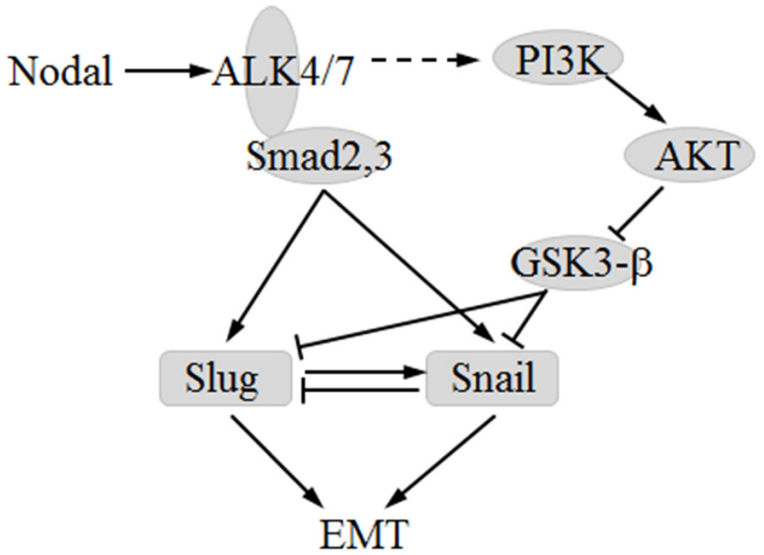

Figure 7. Schematic of the mechanism of Nodal-induced EMT.

comes from Snail its own is abolished, and the transcriptional activity of *Snail* will be up-regulated, which will be more obviously when ALK/Smads pathway is activated. But this up-regulate has no biological effects, because it cannot reflect to protein level. However, Slug can induce its own expression [41]. So the degraded of protein of Slug will suppress the transcriptional activity of *Slug*. So inhibiting PI3k/AKT will suppress the mRNA level of Slug. Furthermore, we demonstrated that the feedback mechanism of Snail and Slug is not only existed in their own regulation but also in their mutual regulation. We proved that Snail can suppress Slug, and Slug can promote Snail (Figure S1). Taken together, we draw the schematic of the mechanism of Nodal-induced EMT (**Figure 7**).

It is a little confusing that EMT is not completely inhibited by blocking the paracrine of Nodal. This suggests that maybe Nodal can enhance the migration capability of tumor cells without secreted to medium. And this is independent on ALK/Smads pathway and PI3k/AKT pathway. A possible explanation is that Nodal is not only cytokine but also has signal protein function. Cytokines are known to signal by interactions with cell-surface receptors which couple to cytoplasmic components that transmit the signal. A growing body of evidence suggests that some cytokines must also act within the cell to exert their complete effect [47, 48]. Although ligand-induced endocytosis of cytokine-receptor complexes traditionally is presumed to function in cellular desensitization and receptor recycling, several cytokines or their receptors contain nuclear localization signals. Once internalized, these cytokine-receptor complexes may be transported into the nucleus. The immunofluorescence microscopy results show that, in B16-pldNodal cells, Nodal was partly located to nucleus (**Figure 2D**). And Nodal is also can be detected in nucleoprotein [9]. So, maybe Nodal has an unknown role that needs to be further studied.

Acknowledgements

National Basic Research Program of China; Contract grant number: No. 2011CB935803 and National Natural Science Foundation of China; Contract grant number: No. 81272311.

Disclosure of conflict of interest

None.

Address correspondence to: Shao-Hui Cai, Department of Pharmacology, College of Pharmacy, Jinan University, Guangzhou 510632, Guangdong, China. Tel: +86 020 85223704; Fax: +86 020 85223704; E-mail: CaiSH5689@163.com; Jun Du, Department of Microbial and Biochemical Pharmacy, School of Pharmaceutical Sciences, Sun Yat-Sen University, Guangzhou 510006, Guangdong, China. Tel: +86 020 39943002; Fax: +86 020 39943002; E-mail: dujun_tg@163.com

References

[1] Smith JR, Vallier L, Lupo G, Alexander M, Harris WA and Pedersen RA. Inhibition of Activin/Nodal signaling promotes specification of human embryonic stem cells into neuroectoderm. Dev Biol 2008; 313: 107-117.

[2] Brennan J, Norris DP and Robertson EJ. Nodal activity in the node governs left-right asymmetry. Genes Dev 2002; 16: 2339-2344.

[3] Wakefield LM and Roberts AB. TGF-beta signaling: positive and negative effects on tumori-

genesis. Curr Opin Genet Dev 2002; 12: 22-29.
[4] Lawrence MG, Margaryan NV, Loessner D, Collins A, Kerr KM, Turner M, Seftor EA, Stephens CR, Lai J, BioResource APC, Postovit LM, Clements JA and Hendrix MJ. Reactivation of embryonic nodal signaling is associated with tumor progression and promotes the growth of prostate cancer cells. Prostate 2011; 71: 1198-1209.
[5] Papageorgiou I, Nicholls PK, Wang F, Lackmann M, Makanji Y, Salamonsen LA, Robertson DM and Harrison CA. Expression of nodal signalling components in cycling human endometrium and in endometrial cancer. Reprod Biol Endocrinol 2009; 7: 122.
[6] Strizzi L, Postovit LM, Margaryan NV, Seftor EA, Abbott DE, Seftor RE, Salomon DS and Hendrix MJ. Emerging roles of nodal and Cripto-1: from embryogenesis to breast cancer progression. Breast Dis 2008; 29: 91-103.
[7] Topczewska JM, Postovit LM, Margaryan NV, Sam A, Hess AR, Wheaton WW, Nickoloff BJ, Topczewski J and Hendrix MJ. Embryonic and tumorigenic pathways converge via Nodal signaling: role in melanoma aggressiveness. Nat Med 2006; 12: 925-932.
[8] Xu G, Zhong Y, Munir S, Yang BB, Tsang BK and Peng C. Nodal induces apoptosis and inhibits proliferation in human epithelial ovarian cancer cells via activin receptor-like kinase 7. J Clin Endocrinol Metab 2004; 89: 5523-5534.
[9] Fu G and Peng C. Nodal enhances the activity of FoxO3a and its synergistic interaction with Smads to regulate cyclin G2 transcription in ovarian cancer cells. Oncogene 2011; 30: 3953-3966.
[10] Lee CC, Jan HJ, Lai JH, Ma HI, Hueng DY, Lee YC, Cheng YY, Liu LW, Wei HW and Lee HM. Nodal promotes growth and invasion in human gliomas. Oncogene 2010; 29: 3110-3123.
[11] Quail DF, Zhang G, Walsh LA, Siegers GM, Dieters-Castator DZ, Findlay SD, Broughton H, Putman DM, Hess DA and Postovit LM. Embryonic morphogen nodal promotes breast cancer growth and progression. PLoS One 2012; 7: e48237.
[12] Vo BT and Khan SA. Expression of nodal and nodal receptors in prostate stem cells and prostate cancer cells: autocrine effects on cell proliferation and migration. Prostate 2011; 71: 1084-1096.
[13] Fang R, Zhang G, Guo Q, Ning F, Wang H, Cai S and Du J. Nodal promotes aggressive phenotype via Snail-mediated epithelial-mesenchymal transition in murine melanoma. Cancer Lett 2013; 333: 66-75.
[14] Leiter U and Garbe C. Epidemiology of melanoma and nonmelanoma skin cancer--the role of sunlight. Adv Exp Med Biol 2008; 624: 89-103.
[15] Postovit LM, Margaryan NV, Seftor EA, Kirschmann DA, Lipavsky A, Wheaton WW, Abbott DE, Seftor RE and Hendrix MJ. Human embryonic stem cell microenvironment suppresses the tumorigenic phenotype of aggressive cancer cells. Proc Natl Acad Sci U S A 2008; 105: 4329-4334.
[16] Greenburg G and Hay ED. Epithelia suspended in collagen gels can lose polarity and express characteristics of migrating mesenchymal cells. J Cell Biol 1982; 95: 333-339.
[17] Zeisberg M and Neilson EG. Biomarkers for epithelial-mesenchymal transitions. J Clin Invest 2009; 119: 1429-1437.
[18] Tse JC and Kalluri R. Mechanisms of metastasis: epithelial-to-mesenchymal transition and contribution of tumor microenvironment. J Cell Biochem 2007; 101: 816-829.
[19] Boulay JL, Dennefeld C and Alberga A. The Drosophila developmental gene snail encodes a protein with nucleic acid binding fingers. Nature 1987; 330: 395-398.
[20] Alberga A, Boulay JL, Kempe E, Dennefeld C and Haenlin M. The snail gene required for mesoderm formation in Drosophila is expressed dynamically in derivatives of all three germ layers. Development 1991; 111: 983-992.
[21] Barrallo-Gimeno A and Nieto MA. The Snail genes as inducers of cell movement and survival: implications in development and cancer. Development 2005; 132: 3151-3161.
[22] Villarejo A, Cortes-Cabrera A, Molina-Ortiz P, Portillo F and Cano A. Differential role of Snail1 and Snail2 zinc fingers in E-cadherin repression and epithelial to mesenchymal transition. J Biol Chem 2014; 289: 930-941.
[23] Chiang C and Ayyanathan K. Characterization of the E-box binding affinity to snag-zinc finger proteins. Mol Biol (Mosk) 2012; 46: 907-914.
[24] Naber HP, Drabsch Y, Snaar-Jagalska BE, ten Dijke P and van Laar T. Snail and Slug, key regulators of TGF-beta-induced EMT, are sufficient for the induction of single-cell invasion. Biochem Biophys Res Commun 2013; 435: 58-63.
[25] Li LL, Jiang GM, Zhang G, Wang H, Fang R and Du J. [Prokaryotic expression and polyclonal antibody preparation of human Nodal mature peptide]. Xi Bao Yu Fen Zi Mian Yi Xue Za Zhi 2011; 27: 880-882.
[26] Zhang H HSC, Cai S H. Development of 2A Peptide-based Strategies for Constructing Multicistronic Expression Vectors. China Biotechnology 2013; 33: 104-108.
[27] Szymczak-Workman AL, Vignali KM and Vignali DA. Verification of 2A peptide cleavage. Cold Spring Harb Protoc 2012; 2012: 255-257.

[28] Szymczak-Workman AL, Vignali KM and Vignali DA. Design and construction of 2A peptide-linked multicistronic vectors. Cold Spring Harb Protoc 2012; 2012: 199-204.
[29] Vellonen KS, Honkakoski P and Urtti A. Substrates and inhibitors of efflux proteins interfere with the MTT assay in cells and may lead to underestimation of drug toxicity. Eur J Pharm Sci 2004; 23: 181-188.
[30] Jiang GM, He YW, Fang R, Zhang G, Zeng J, Yi YM, Zhang S, Bu XZ, Cai SH and Du J. Sodium butyrate down-regulation of indoleamine 2, 3-dioxygenase at the transcriptional and post-transcriptional levels. Int J Biochem Cell Biol 2010; 42: 1840-1846.
[31] Wang H, Wang HS, Zhou BH, Li CL, Zhang F, Wang XF, Zhang G, Bu XZ, Cai SH and Du J. Epithelial-mesenchymal transition (EMT) induced by TNF-alpha requires AKT/GSK-3beta-mediated stabilization of snail in colorectal cancer. PLoS One 2013; 8: e56664.
[32] Brandl M, Seidler B, Haller F, Adamski J, Schmid RM, Saur D and Schneider G. IKK(alpha) controls canonical TGF(ss)-SMAD signaling to regulate genes expressing SNAIL and SLUG during EMT in panc1 cells. J Cell Sci 2010; 123: 4231-4239.
[33] Saka Y, Hagemann AI, Piepenburg O and Smith JC. Nuclear accumulation of Smad complexes occurs only after the midblastula transition in Xenopus. Development 2007; 134: 4209-4218.
[34] Wu Y, Fu Y, Zheng L, Lin G, Ma J, Lou J, Zhu H, He Q and Yang B. Nutlin-3 inhibits epithelial-mesenchymal transition by interfering with canonical transforming growth factor-beta1-Smad-Snail/Slug axis. Cancer Lett 2014; 342: 82-91.
[35] Medici D, Potenta S and Kalluri R. Transforming growth factor-beta2 promotes Snail-mediated endothelial-mesenchymal transition through convergence of Smad-dependent and Smad-independent signalling. Biochem J 2011; 437: 515-520.
[36] Zhou BP, Deng J, Xia W, Xu J, Li YM, Gunduz M and Hung MC. Dual regulation of Snail by GSK-3beta-mediated phosphorylation in control of epithelial-mesenchymal transition. Nat Cell Biol 2004; 6: 931-940.
[37] Dominguez D, Montserrat-Sentis B, Virgos-Soler A, Guaita S, Grueso J, Porta M, Puig I, Baulida J, Franci C and Garcia de Herreros A. Phosphorylation regulates the subcellular location and activity of the snail transcriptional repressor. Mol Cell Biol 2003; 23: 5078-5089.
[38] Gharbi SI, Zvelebil MJ, Shuttleworth SJ, Hancox T, Saghir N, Timms JF and Waterfield MD. Exploring the specificity of the PI3K family inhibitor LY294002. Biochem J 2007; 404: 15-21.
[39] Ojeda L, Gao J, Hooten KG, Wang E, Thonhoff JR, Dunn TJ, Gao T and Wu P. Critical role of PI3K/Akt/GSK3beta in motoneuron specification from human neural stem cells in response to FGF2 and EGF. PLoS One 2011; 6: e23414.
[40] Peiro S, Escriva M, Puig I, Barbera MJ, Dave N, Herranz N, Larriba MJ, Takkunen M, Franci C, Munoz A, Virtanen I, Baulida J and Garcia de Herreros A. Snail1 transcriptional repressor binds to its own promoter and controls its expression. Nucleic Acids Res 2006; 34: 2077-2084.
[41] Sakai D, Suzuki T, Osumi N and Wakamatsu Y. Cooperative action of Sox9, Snail2 and PKA signaling in early neural crest development. Development 2006; 133: 1323-1333.
[42] Boerner BP, George NM, Targy NM and Sarvetnick NE. TGF-beta superfamily member Nodal stimulates human beta-cell proliferation while maintaining cellular viability. Endocrinology 2013; 154: 4099-4112.
[43] He Z, Jiang J, Kokkinaki M and Dym M. Nodal signaling via an autocrine pathway promotes proliferation of mouse spermatogonial stem/progenitor cells through Smad2/3 and Oct-4 activation. Stem Cells 2009; 27: 2580-2590.
[44] Sun J, Liu SZ, Lin Y, Cao XP and Liu JM. TGF-beta promotes glioma cell growth via activating Nodal expression through Smad and ERK1/2 pathways. Biochem Biophys Res Commun 2014; 443: 1066-1072.
[45] Munir S, Xu G, Wu Y, Yang B, Lala PK and Peng C. Nodal and ALK7 inhibit proliferation and induce apoptosis in human trophoblast cells. J Biol Chem 2004; 279: 31277-31286.
[46] Zhang YQ, Sterling L, Stotland A, Hua H, Kritzik M and Sarvetnick N. Nodal and lefty signaling regulates the growth of pancreatic cells. Dev Dyn 2008; 237: 1255-1267.
[47] Jans DA and Hassan G. Nuclear targeting by growth factors, cytokines, and their receptors: a role in signaling? Bioessays 1998; 20: 400-411.
[48] Johnson HM, Torres BA, Green MM, Szente BE, Siler KI, Larkin J 3rd and Subramaniam PS. Cytokine-receptor complexes as chaperones for nuclear translocation of signal transducers. Biochem Biophys Res Commun 1998; 244: 607-614.

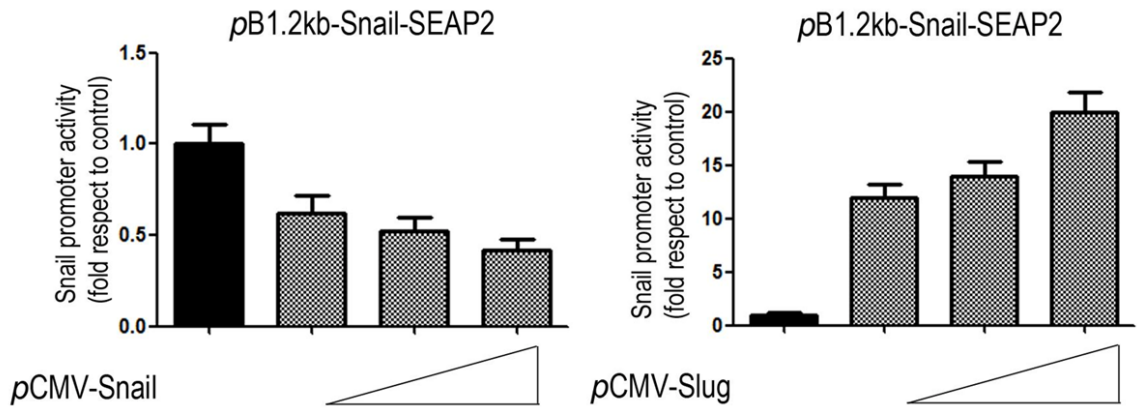

Figure S1. Activity of the pB1.2kb-Snail-SEAP2 was determined in B16 cells by transient transfection; when indicated, Snail or Slug was co-transfected at several concentrations. After transfection, cells were incubated for 24 hours, and promoter activities were measured. Black bars correspond to activity of promoter in the absence of Snail1 or Slug co-transfection.